Supporting Information

Cellmer *et al.* 10.1073/pnas.0806154105

SI Text

Additional Measurements. Fig. S1 shows equilibrium and kinetic quantum yields at each temperature and ethylene glycol concentration. Quantitative agreement between the 2 measurements shows the absence of missing kinetic amplitude.

Thermodynamic Measurements of Villin Folding in Glucose and Glycerol. Fig. S2 shows equilibrium unfolding curves measured by circular dichroism and fluorescence for villin at different concentrations of glucose and glycerol. With the exception of the viscogen, the solution conditions and measurement parameters were the same as those described in the text for solutions containing villin in ethylene glycol. The same 2-state fitting procedure was also used to extract thermodynamic parameters from the fluorescence data, including the free energies shown in Table S1.

Relaxation Time as a Function of Viscosity Without Scaling of Free Energies. Figure S3 shows the experimental relaxation times as a function of viscosity along with fits from the theoretical model. The free energy surfaces used to calculate the theoretical times were not scaled. The internal viscosity (σ,) calculated from the model is nearly independent of temperature.

Comparisons of Viscosity Dependence from Simulations and Experiments. Fig. S4–S6 compare experimental with simulation results on the viscosity dependence of folding rates from previous studies.

Possible Effect of Position-Dependent Diffusion Coefficient on Relative Folding Rates for 2-State Proteins. Fig. S3*B* shows that $\gamma(Q)$ decreases by <10-fold for the fully folded ($Q = 1$) protein relative to the fully unfolded protein ($Q = 0$). This relatively small decrease is consistent with the success of the Ising-like model of Muñoz, Henry, and Eaton in predicting folding rates for 2-state proteins. In applying this model, it was assumed that the diffusion coefficient is independent of the reaction coordinate (either the fraction of native contacts or the number of ordered residues) and is the same for all proteins. Although the model predicts these rates with remarkable accuracy (1, 2) (Fig. S7), there are substantial differences between the predicted and observed rates. Therefore, one might ask whether some of the deviations between observed and predicted rates arise from variations in the diffusion coefficient. One possibility is that the deviations arise from differences in hydrophobicity, with the more hydrophobic sequences expected to be "stickier," and therefore result in deeper local energy minima and a smaller diffusion coefficient. However, no correlation was observed between the hydrophobicity calculated in several different ways and the deviations (E.R.H. and W.A.E. unpublished results). Another possibility is that the free energy barrier top appears at different positions along the reaction coordinate, as judged by the relative sensitivity of the folding rate and equilibrium constant to denaturant, determined from the ratio of the slopes m^*_f/m_{eq}, with late transition states corresponding to more compact structures and therefore increased internal friction. Fig. S8*A* shows no correlation. Fig. S8*B* shows the absolute contact order as the predictor of rates, again with no significant correlation.

Although the Ising-like model is much oversimplified and the contact order is only an approximate determinant of folding rates, the lack of any correlation of rates with properties that are expected to affect the diffusion coefficient is consistent with the notion that the underlying energy landscape for these proteins is relatively smooth and that the variation in the diffusion coefficient along the reaction coordinate is also small, as found in fitting Eq. **3** of the main text to the data in Fig. 2*B*.

Analysis of Kinetics in Terms of Mean First Passage Times. To investigate the kinetics in more detail, we calculated mean first-passage times between minima of the free energy surface (Fig. S9). The kinetics of hopping along the free energy surface of Fig. 3*A* are described by the master equation:

$$\frac{d\mathbf{p}}{dt} = \mathrm{K}\mathbf{p}, \qquad [1]$$

where $\mathbf{p}$ is a column vector containing the time-dependent populations at each value of the reaction coordinate, and $\mathbf{K}$ is the tri-diagonal rate matrix describing the kinetics of interconversion between adjacent values (Q_i, $Q_{i \pm 1}$) of the reaction coordinate. The set of mean first-passage times corresponding to a specific sink state Q_j for all initial states $Q_i \neq Q_j$ (comprising a vector τ_j) is most easily computed using the following relation (3):

$$\tilde{\mathbf{K}}\tau_j = -1 \qquad [2]$$

where $\tilde{\mathbf{K}}$ is the rate matrix with row and column j removed, and $-\mathbf{1}$ represents a column vector all components of which are -1.

The calculated mean first passage times for transitions across the 2 barriers show that the lack of a temperature dependence of σ obtained from the free energy profiles results from the fact that the relaxation times for the folding transition are not controlled by the barrier at $Q = 0.12$ under any set of experimental conditions. At low temperature, where one would expect the folding rate to be determined by crossing the $Q = 0.12$ barrier, the time for crossing $Q = 0.56$ barrier is the same when the hopping parameter $\gamma(Q)$ is coordinate-independent. This is because the attempt frequency from the $Q = 0$ minimum is much higher than that from the $Q = 0.32$ minimum. When $\gamma(Q)$ is scaled according to Eq. **3** main text, the first passage times from the unfolded to folded state are dominated by the time required to cross the barrier at $Q = 0.56$ at all temperatures. At low temperatures the mean first passage times from the folded to the unfolded state are determined by the time required to cross the barrier at $Q = 0.12$ but, because the measured relaxation time is primarily determined by the folding rate, the viscosity dependence for the crossing of this barrier is not observed experimentally. At 70° C, where the relaxation time is primarily determined by the unfolding rate, the relaxation time is again determined primarily by the time required to cross the $Q = 0.56$ peak. Because the barrier at $Q = 0.12$ does not determine the folding rates under any set of experimental conditions, it is not possible to successfully fit the temperature dependence of the internal friction with the profiles of Fig. 3*A* without scaling the free energies.

1. Muñoz V, Eaton WA (1999) A simple model for calculating the kinetics of protein folding from three-dimensional structures. *Proc Natl Acad Sci USA* 96:11311–11316.

2. Henry ER, Eaton WA (2004) Combinatorial modeling of protein folding kinetics: Free energy profiles and rates. *Chem Phys* 307:163–185.

3. Szabo A, Schulten K, Schulten Z (1980) First passage time approach to diffusion controlled reactions. *J Chem Phys* 72:4350–4357.
4. Qiu LL, Hagen SJ (2004) Internal friction in the ultrafast folding of the tryptophan cage. *Chem Phys* 307:243–249.
5. Zagrovic B, Pande V (2003) Solvent viscosity dependence of the folding rate of a small protein: Distributed computing study. *J Comp Chem* 24:1432–1436.
6. Best RB, Hummer G (2006) Diffusive model of protein folding dynamics with Kramers turnover in rate. *Phys Rev Lett* 96:228104.

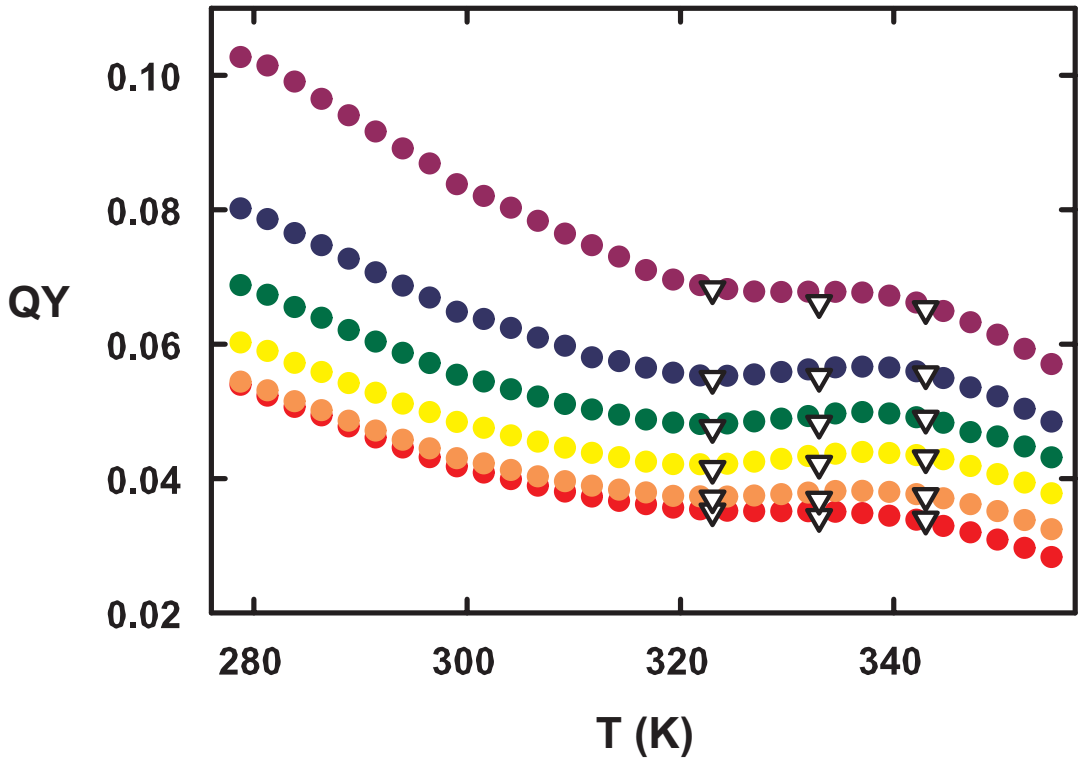

Fig. S1. Equilibrium (colored circles) and kinetic quantum yields (black and white triangles) as a function of ethylene glycol (EG) concentration. Red circles represent data with no EG. wt/wt EG: orange, 11%; yellow, 22%; green, 32%; blue, 43%; violet, 53%.

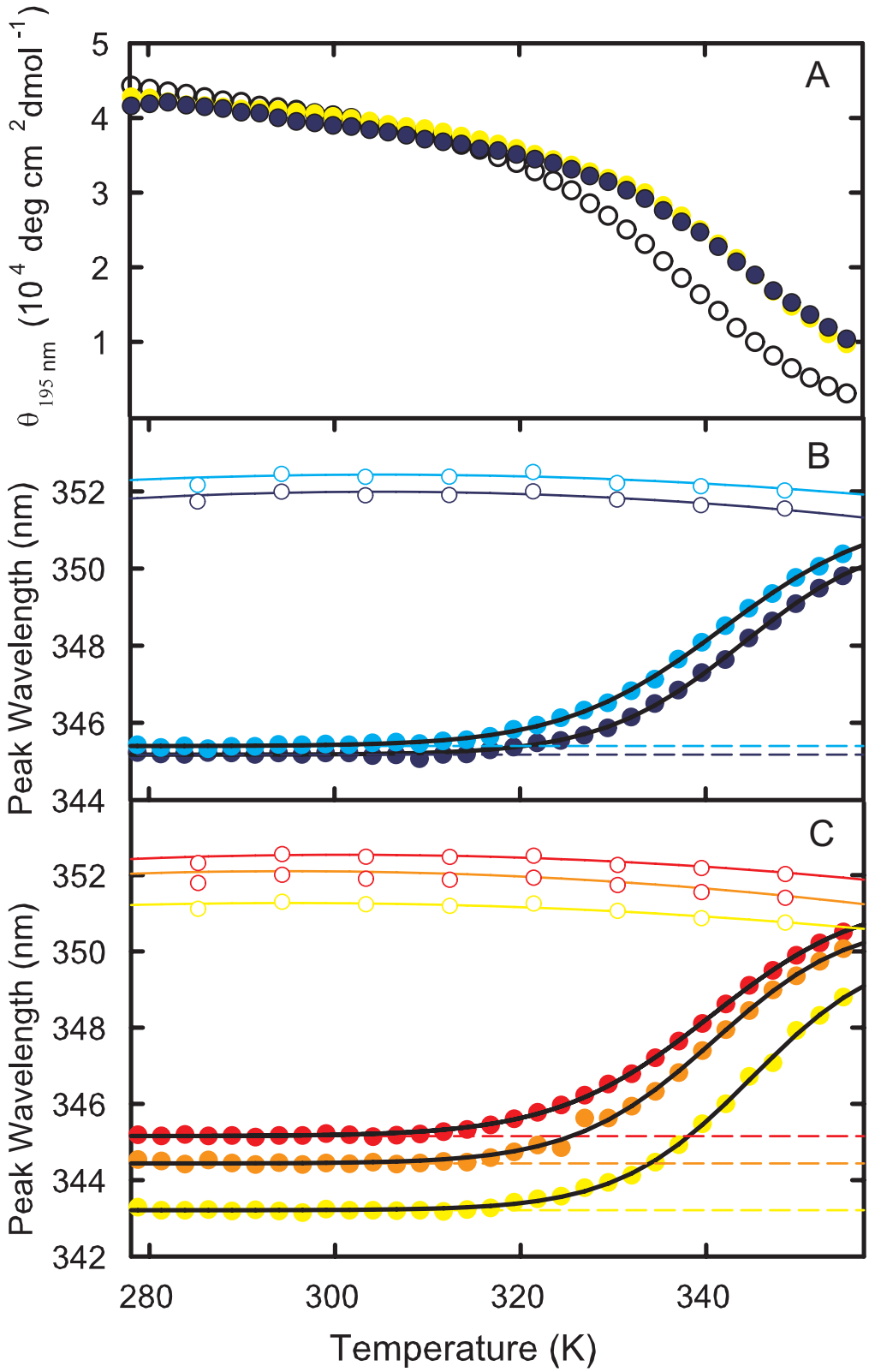

Fig. S2. Equilibrium thermal unfolding measured by natural circular dichroism and tryptophan fluorescence. (*A*) Ellipticity at 195 nm versus temperature with no viscogen (open circles), 50% wt/wt glycerol (yellow), and 20% wt/wt glucose (dark blue). (*B*) Peak wavelength of tryptophan fluorescence versus temperature at 10% glucose (cyan) and 20% glucose (blue). See main text for fitting procedure. (*C*) Peak wavelength of tryptophan fluorescence versus temperature at 15% glycerol (red), 30% glycerol (orange), and 50% glycerol (yellow).

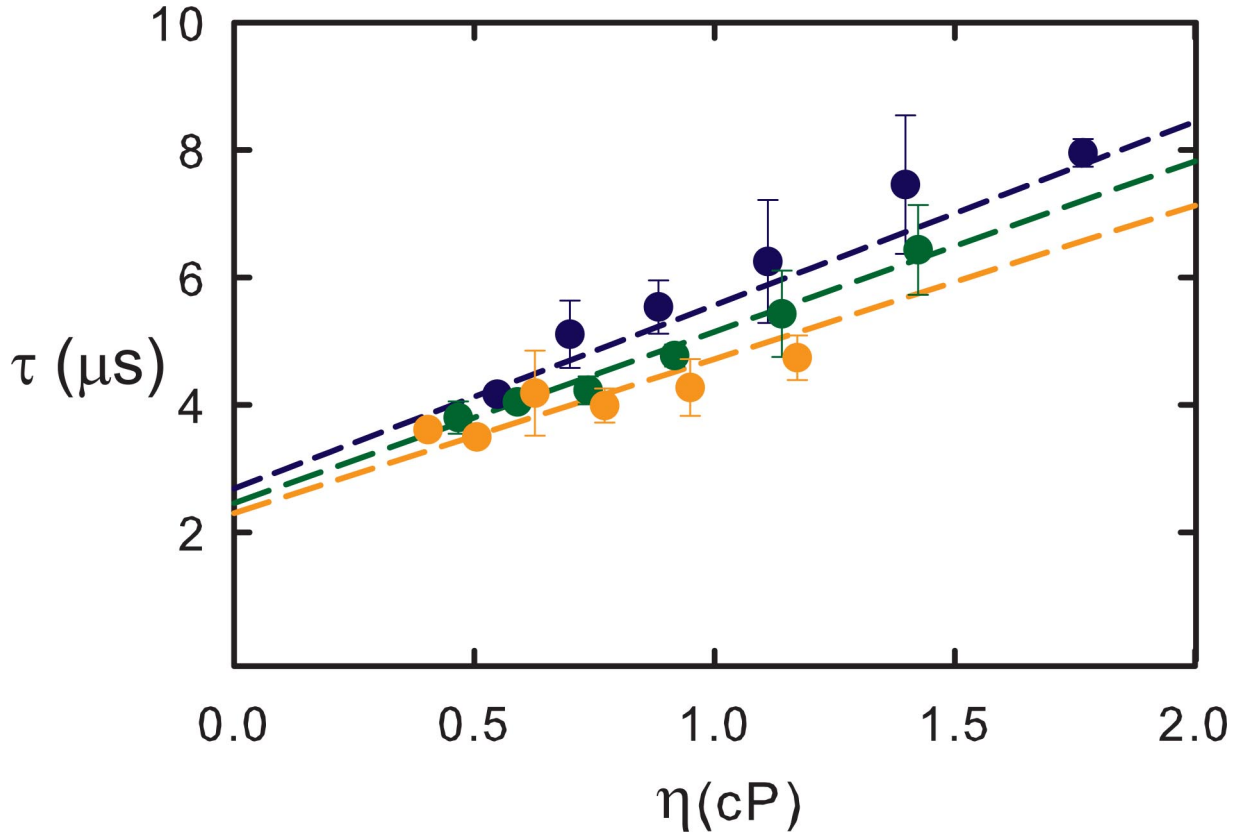

Fig. S3. Theoretical relaxation time versus viscosity at 50° C (blue), 60° C (green), and 70°C (orange) without scaling the free energy profiles. The points are the data. The dashed curves are the best fit using using Eq. **3** (main text) and the Ising-like model with no scaling of the free energy profiles, with α constrained to be zero and $\beta = 2.1 \pm 0.2$, corresponding to a 68% interval, $\Delta\chi^2 = 1$, Γ (50° C) $= 6.58 \pm 0.30 \times 10^7$ s^{-1} cP, Γ (60° C) $= 1.21 \pm 0.06 \times 10^8$ s^{-1} cP, and Γ (70° C) $= 1.67 \pm 0.09 \times 10^8$ s^{-1} cP. The corresponding values of σ obtained by fitting the theoretical curves with Eq. **2** of the main text are: σ (50° C) $= 0.93$, σ (60° C) $= 0.92$, σ (70° C) $= 0.95$.

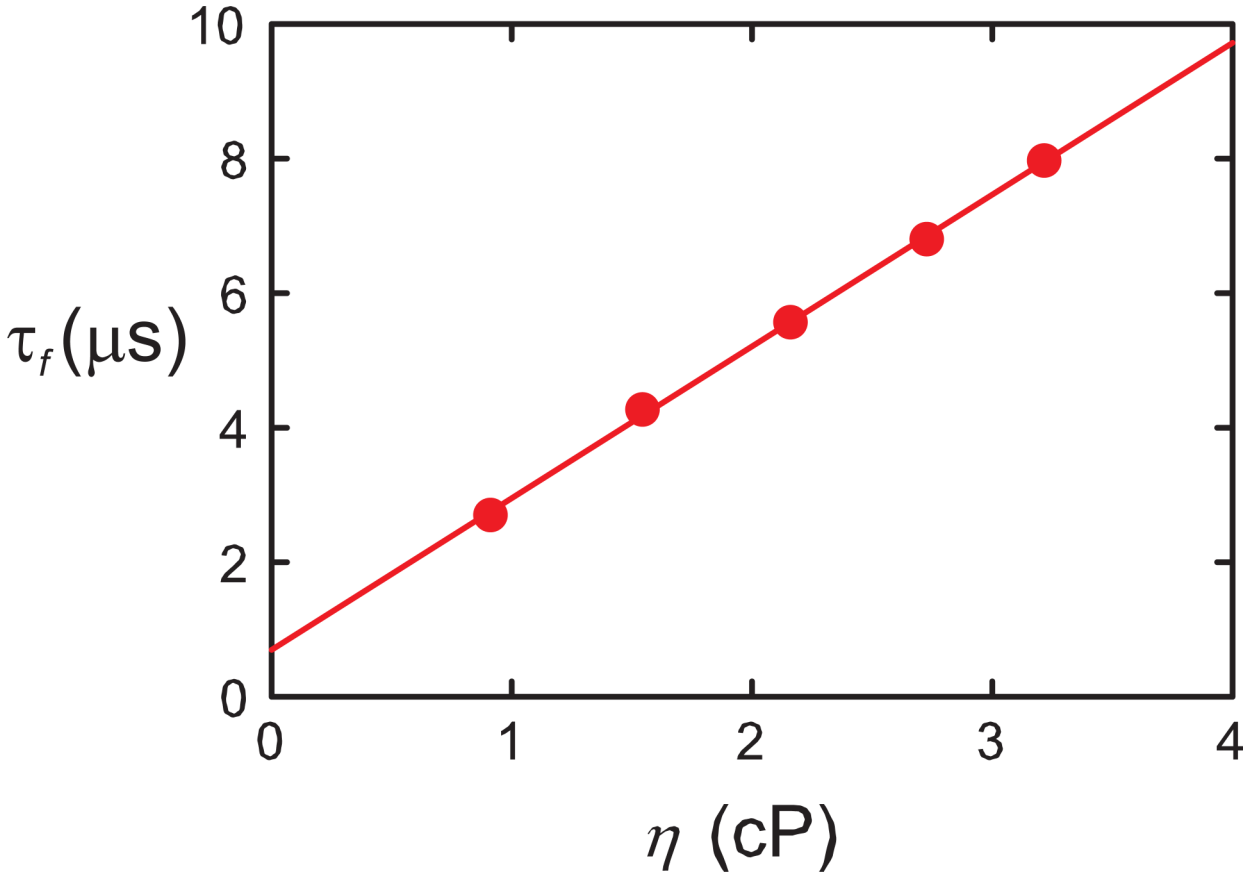

Fig. S4. Data (circles) of Qiu and Hagen for the viscosity dependence of the unfolding/refolding relaxation time from temperature jump experiments on the 20-residue Trp cage at 298 K (4). Fitting to Eq. **2** of main text (straight line) gives $\sigma = 0.28 \pm 0.06$ cP and $B = 0.44 \pm 0.01$ cP/μs.

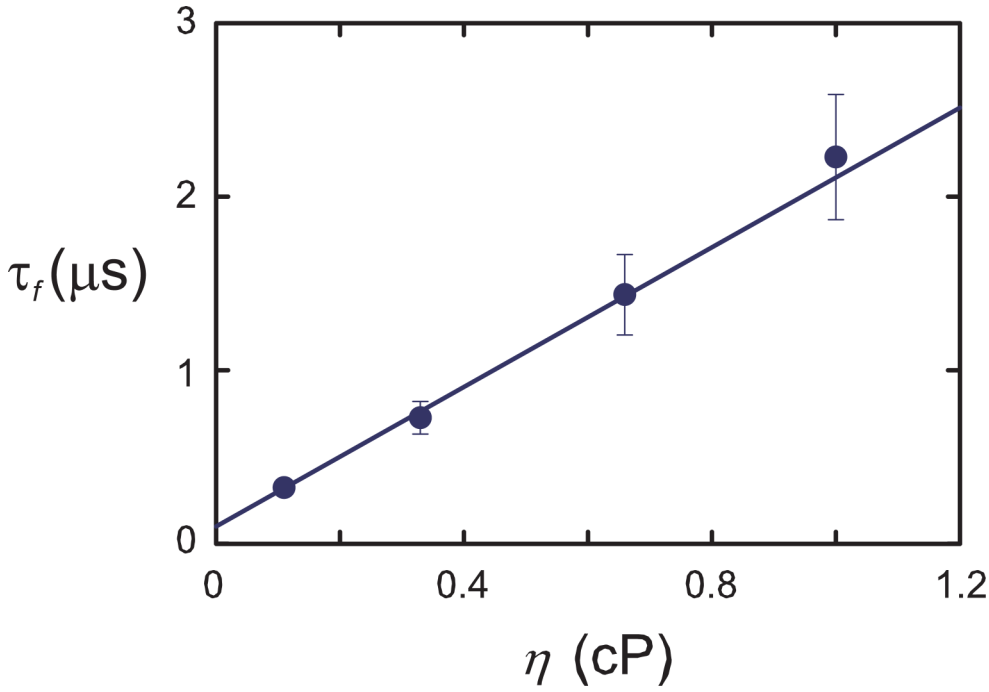

Fig. S5. Data (circles) of Zagrovic and Pande for the viscosity dependence of the folding time for the 20-residue Trp cage from Langevin simulations at 300 K (assuming collision frequency of 91/ps corresponds to 1 cP) (5). Fitting to Eq. **2** of main text (straight line) gives $\sigma = 0.05 \pm 0.03$ cP and $B = 0.50 \pm 0.06$ cP/μs.

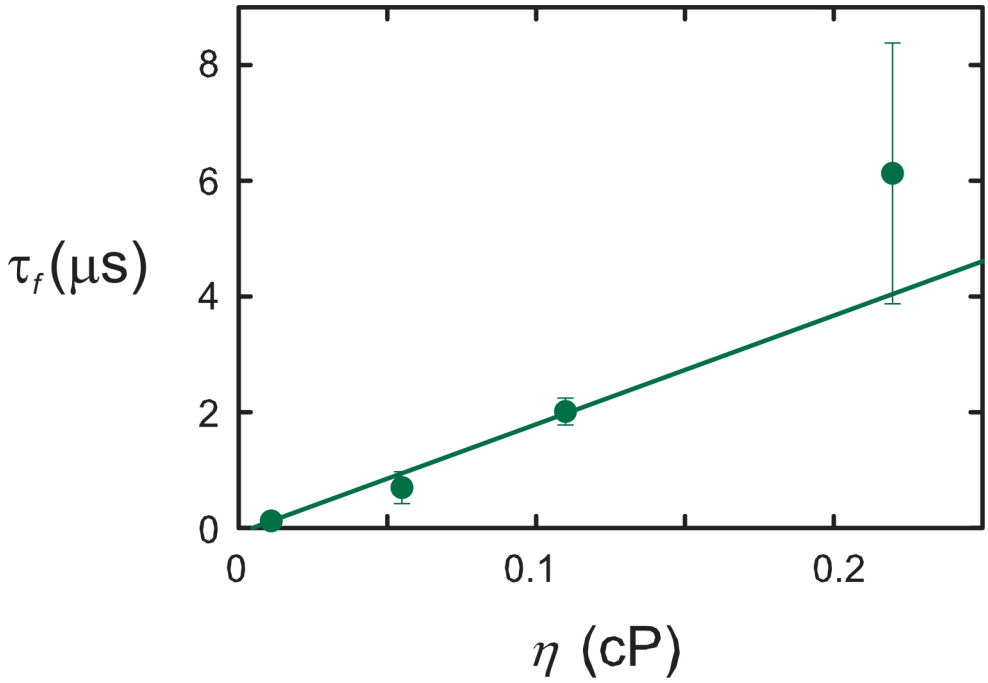

Fig. S6. Data (circles) of Best and Hummer for the viscosity dependence of the folding time for a bead model of a 47-residue 3-helix bundle protein from Langevin simulations at 292 K (assuming collision frequency of 91/ps corresponds to 1 cP) (6). Fitting to Eq. **2** of main text (straight line) gives $\sigma = -0.0047 \pm 0.0015$ cP and $B = 0.053 \pm 0.006$ cP/μs.

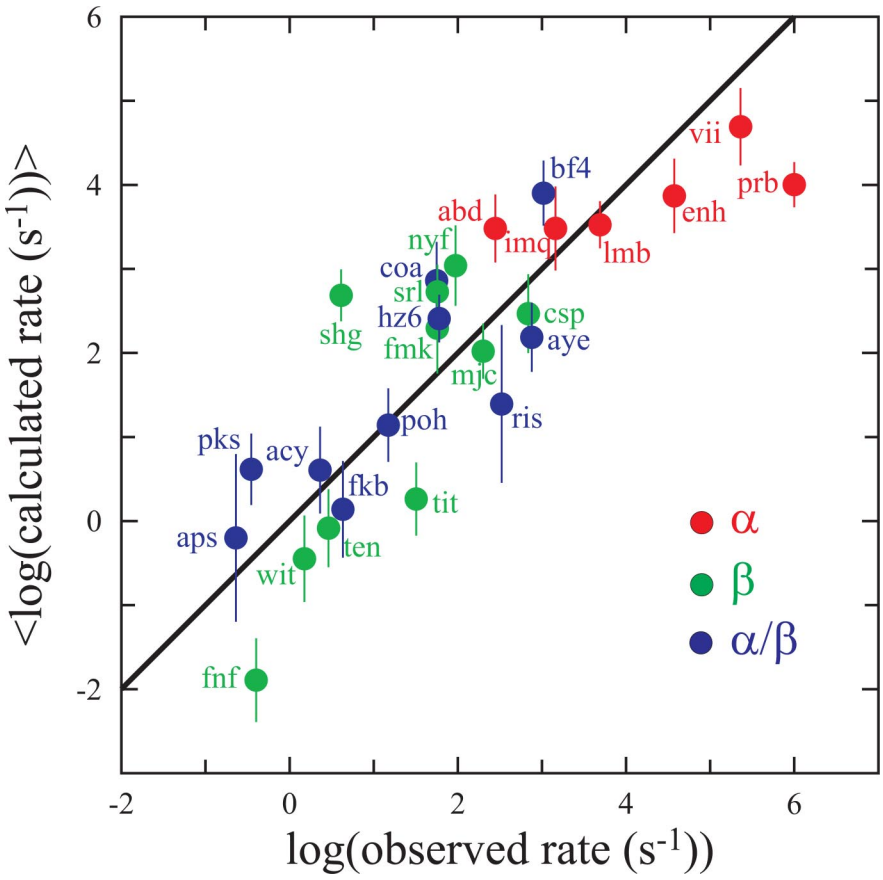

Fig. S7. Comparison of measured folding rates and rates calculated by Henry and Eaton (Fig. 7a) assuming the same value of the hopping parameter, γ (Eq. **3** of main text) for all proteins (2).

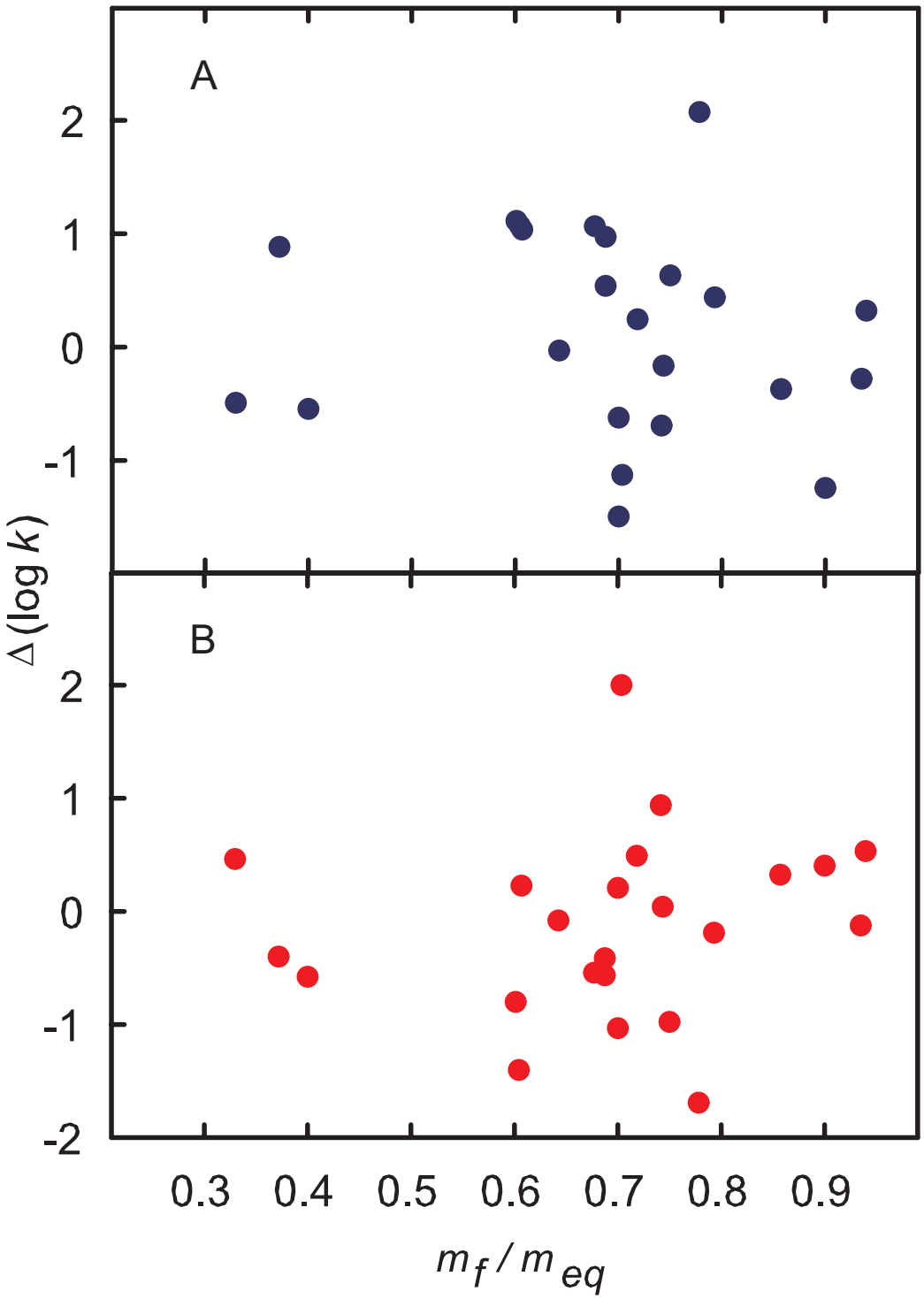

Fig. S8. Deviations from predicted rates. (*A*) Difference between the logarithm of the calculated rates and the logarithm of the experimentally measured rates from Fig. 7*a* in ref (2). The experimentally measured rates were first plotted against the rates from an Ising-like model calculated by Henry and Eaton (2), and the data were fitted to a straight line. Deviations of the experimentally measured rates and the linear fit were then plotted against the folding *m* value ($m_f^{\ddagger}$) divided by the sum of the folding and unfolding *m* values (m_{eq}). (*B*) Difference between the logarithm of the experimentally measured rates and the logarithm of the rates predicted from the least-squares line of a rate-contact order plot (figure 9a in ref 2.). In *A*, differences between the calculated and measured were plotted against the ratio $m_f^{\ddagger}/m_{eq}$.

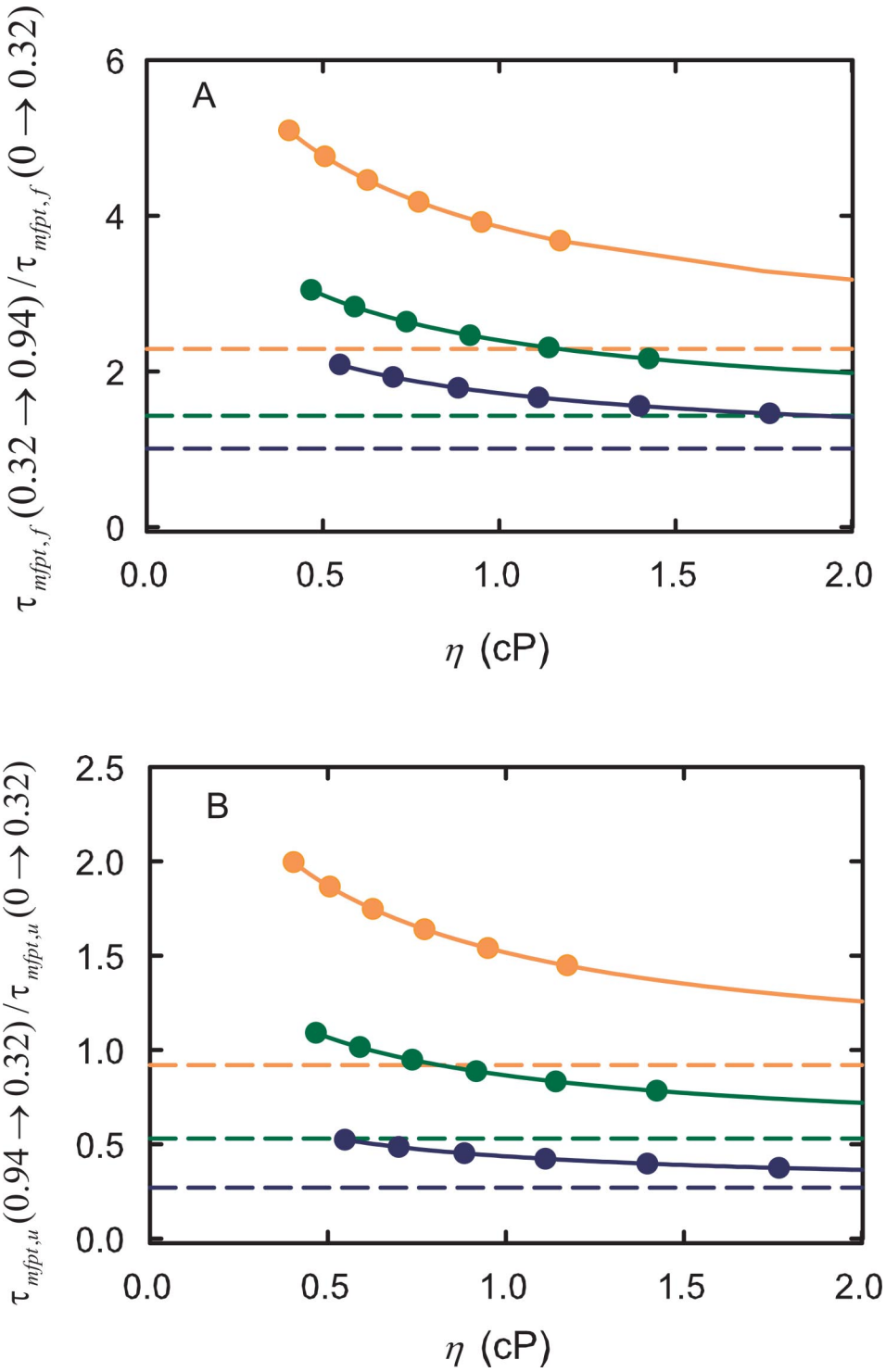

Fig. S9. Ratio of first passage times for crossing the barriers at $Q = 0.56$ and $Q = 0.12$ obtained from fits using the Ising-like model. (*A*) The ratio of the first passage time from the minimum at $Q = 0.32$ to the folded state ($Q = 0.94$) to that from the unfolded state to the minimum at $Q = 0.32$ are shown at 50° C (blue), 60° C (green), 70° C (orange). The values obtained for coordinate-dependent internal viscosity, shown as continuous lines (points are for the experimental conditions in Fig. 2) and those obtained for coordinate-independent internal viscosity (dashed lines) are >1 at all temperatures, demonstrating that the time required to pass over the barrier at $Q = 0.56$ contributes significantly to the folding rates under all conditions. When the viscosity is coordinate-dependent, the mean first-passage time over this barrier at low external viscosity is at least 2-fold larger than for crossing the low Q barrier, so the barrier at $Q = 0.12$ does not determine the folding rates. (*B*) The ratio of the mean first passage time from the folded state ($Q = 0.94$) to the minimum at $Q = 0.32$ to that from the minimum at $Q = 0.32$ to the unfolded state at $Q = 0$ are shown 50° C (blue), 60° C (green), 70° C (orange) using lines and symbols identical to (*A*).

Table S1. Thermodynamic and kinetic parameters for villin folding at 60 °C in glycerol and glucose.

Viscogen	Weight, %	ΔG_{uf} (60°C), cal/mol	η, cP	τ, μs	
				Measured	Corrected
None	—	330 ± 150	0.47	3.80 ± 0.44	—
Glucose	10	800 ± 175	0.51	4.45 ± 0.40	3.70 ± 0.55
Glucose	20	1,050 ± 240	0.80	5.11 ± 0.16	4.25 ± 0.54
Glycerol	15	760 ± 90	0.65	4.72 ± 0.41	4.13 ± 0.75
Glycerol	30	850 ± 110	0.96	4.81 ± 0.45	4.47 ± 0.69
Glycerol	50	1,160 ± 90	1.86	8.0 ± 1.8	6.4 ± 2.3